A Bin Packing Approach to Minimize Charging Cost for Electric Bus Fleets

Daniel Mortensen, Jacob Gunther, Greg Droge

Abstract—As transit authorities begin adopting Battery Electric Buses (BEBs), they must address the challenge of extended battery charging sessions while maintaining fixed bus schedules and managing the cost of energy. This paper proposes a novel technique for minimizing the monthly cost of energy for operating electric bus fleets in the presence of time-varying uncontrolled loads. The charging problem is cast as a constrained bin packing problem and expressed as a mixed integer linear program (MILP). Among other things, we show that the proposed method significantly decreases demand on power infrastructure by temporally balancing the loads from buses with uncontrolled loads.

Index Terms—Battery Electric Buses, Cost Minimization, Bin Packing, Mixed Integer Linear Program

I. INTRODUCTION

Battery powered electric motors offer many benefits over the internal combustion engine [1] such as reduced maintenance [2], zero emissions [3], and access to renewable energy [4], which have caused many transit authorities to adopt battery powered electric buses (BEBs).

Despite their benefits, the transition to BEBS must address the challenge of extended refuel times. When a bus fueled by diesel or compressed natural gas (CNG) runs low on fuel, the bus may refuel in five to ten minutes, whereas an electric bus may require several hours, presenting logistical challenges for bus fleets. Therefore, maintaining a route schedule while staying charged is a primary concern that BEBs face, and requires careful planning that models how batteries discharge along routes, how long BEBs must charge, and limitations on the number of chargers.

One way in which charge times may be reduced is by charging a bus while it is in motion through dynamic charging. There are a number of ways to do this, including overhead [5] and inductive charging [6] [7]. An overhead charging scenario allows the bus to charge on overhead power lines while in motion. Inductive charging relies on specialized hardware in the roads that transfers energy to buses that pass overhead. Both methods remove the need to stop for service and allow an electric vehicle to stay in service indefinitely. Unfortunately, both methods require extensive infrastructure [8] that may not be available, or is cost prohibitive to install.

In the absence of infrastructure, [9] and [10] have proposed methods that exchange depleted batteries for fresh ones. Such a method would eliminate both the logistical challenges of planning and the infrastructure dependence of dynamic charging. The only drawback, is that BEBs are not built with battery exchanges in mind, therefore the task can require specialized hardware, technical expertise, or automation, all of which add complexity and cost.

One charge option that avoids both the infrastructure demands of dynamic charging and the technical difficulties of battery swapping is stationary charging, which plans rest periods into a bus's schedule during which that bus can charge. Stationary charging is the least invasive form of bus charging because it only requires charging hardware at specific locations and makes no exchanges to bus batteries. Prior work in this area addresses a number of problems, including distributed charging networks [11], bus availability, environmental impact [12], route scheduling [13], battery health [14], the cost of electricity [15], and the cost of charging infrastructure [16].

One drawback to using a stationary charging solution is that it does require significant rest periods for charging. One way to decrease the charge intervals is to use high power chargers, which deliver more energy in a smaller period of time. However doing so places large power demands on electrical infrastructure [17] which may result in problems with network reliability [18] and require additional maintenance and upgrades, which increase the cost of energy [19]. An effective charge plan must therefore balance the need to charge quickly with the desire to maintain a low power profile [20].

The authors of [21] and [22] propose simple, heuristic approaches to reduce power demands from BEB fleets. Work done by [23] uses a mixed integer linear program (MILP) to solve for a solution, which addresses both when buses should charge, and where they should deploy. Finally, a paper by [24] provides a MILP framework for minimizing the cost of demand power and both [25] and [26] minimize the cost from time of use tariffs. Each of the aforementioned methods focus on demand power in relation to electric bus fleets, but do not account for external activity on the grid, such as effects from electric trains, renewable energy devices, or other utilities which we refer to as "uncontrolled loads".

In this paper, the uncontrolled load profile comes from historical data provided by the Utah Transit Authority in Salt Lake City which describes the power demands for an electric train as it passes through the station. In practice, buses would share a single meter with the train. If buses were to charge at high rates while the train drew power from the grid to accelerate, the resulting 15-minute average power would become significant, increasing the monthly cost.

This paper considers a traditional scenario where each bus begins the day in the station and spends the day either on-route or in the station. Buses on route are considered unavailable and cannot charge until that bus returns to the station. For

such a scenario, we develop a planning method to manage bus charging by viewing the charge problem in a bin packing context [27] in a way that minimizes the joint power use from the bus fleet and uncontrolled loads while yielding a precise time schedule for charging.

The rest of this paper is organized as follows: Section II discusses the basic problem formulation, Section III discusses linear constraints that govern the behavior and limitations of the rate of charge. Section IV discusses how to incorporate uncontrolled loads into the optimization framework. Section V explains how the objective function is formed, and Section VI discusses performance.

II. Bus Availability and Resource Contention

The charge scheduling framework described in this paper is formulated as a constrained optimization problem that can be solved as a Mixed Integer Linear Program (MILP) of the form

$$\min_{\mathbf{y}} \mathbf{y}^T \mathbf{v} \text{ subject to} \qquad (1)$$
$$\tilde{A}\mathbf{y} = \tilde{\mathbf{b}}, \ A\mathbf{y} \leq \mathbf{b},$$

along with some integer constraints on elements of $\mathbf{y}$, where $\mathbf{y}$, $\tilde{A}$, A, and $\mathbf{v}$ represent the solution vector, equality and inequality constraints, and cost vector respectively. In this paper, $\mathbf{y}$ is comprised of several variables, and is expressed as

$$\mathbf{y} = \begin{bmatrix} \boldsymbol{\sigma} \\ \mathbf{c} \\ \mathbf{s} \\ \mathbf{h} \\ \mathbf{k} \\ \mathbf{r} \\ \mathbf{g} \\ \mathbf{p} \\ \mathbf{l} \\ q_{\text{on}} \\ q_{\text{all}} \end{bmatrix}, \qquad (2)$$

where $\boldsymbol{\sigma}$ describes on which charger a bus will charge, $\mathbf{c}$ and $\mathbf{s}$ describe time intervals over which buses charge, $\mathbf{h}$ gives the bus state of charge, $\mathbf{k}$, $\mathbf{r}$ and $\mathbf{p}$ are used to discretize the effects from $\mathbf{c}$ and $\mathbf{s}$, $\mathbf{g}$ is a slack variable for converting the effects of charging from continuous time to discrete intervals, $\mathbf{l}$ is another slack variable that prevents two buses from simultaneously being assigned to the same charger, and q_{on} and q_{all} represent maximum average power values that are used to compute the monthly cost of power.

The cost function in (1) will be designed to model a realistic billing structure used by [28] and will minimize the cost in the presence of uncontrolled loads. Additionally, the constraints are designed to incorporate bus schedules, limit bus state of charges, and include a linear charge model calibrated on data from the Utah Transit Authority.

A. Setup

A solution to the bus charge problem includes both temporal and categorical information. The temporal aspect shows when and for how long a bus should charge, and is represented graphically as increasing from left to right. The vertical axis represents each category as a bus and shows how each bus charges over time as shown in Fig. 2.

Each bus follows a schedule of arrival and departure times, where the ith bus's j^{th} stop begins at arrival time a_{ij} and terminates at departure time d_{ij} (see Fig. 1). A bus can be assigned to charge anytime the bus is in the station, such that the charge start time, c_{ij}, is greater than or equal to a_{ij}, and the charge stop time, s_{ij}, is less than the departure time d_{ij}, as shown in Fig. 1. In the context of a MILP, the arrival and departure times a_{ij} and d_{ij} are known ahead of time and charge times c_{ij} and s_{ij} are optimization variables.

B. Constraints

The relationship between the arrival, departure, and charge intervals for the ith bus at the jth stop can be expressed as a set of inequality constraints such that

$$\begin{aligned} a_{ij} &\leq c_{ij} \\ c_{ij} &\leq s_{ij} \\ s_{ij} &\leq d_{ij}. \end{aligned} \qquad (3)$$

These constraints can be rewritten such that the optimization variables are on the left, the known parameters are on the right, and the relationship is "less than" (or standard form) such that

$$\begin{aligned} -c_{ij} &\leq -a_{ij} \\ c_{ij} - s_{ij} &\leq 0 \\ s_{ij} &\leq d_{ij}. \end{aligned} \qquad (4)$$

Standard form is preferred because it is required by most solvers. Having the optimization variables on the left also allows the expression to be written using matrix notation as

$$\begin{bmatrix} -1 & 0 \\ 1 & -1 \\ 0 & 1 \end{bmatrix} \begin{bmatrix} c_{ij} \\ s_{ij} \end{bmatrix} \leq \begin{bmatrix} -a_{ij} \\ 0 \\ d_{ij} \end{bmatrix}. \qquad (5)$$

However, because all constraints must follow the form $A\mathbf{y} = \mathbf{b}$ as shown in (1), (5) is expressed in terms of $\mathbf{y}$ such that

$$\begin{bmatrix} -1_{ij}^c & 0 & \dots & 0 \\ 1_{ij}^c & 0 & \dots & -1_{ij}^d \\ 0 & 0 & \dots & 1_{ij}^d \end{bmatrix} \mathbf{y} \leq \begin{bmatrix} -a_{ij} \\ 0 \\ d_{ij} \end{bmatrix} \ \forall i, j \qquad (6)$$
$$A_1 \mathbf{y} \leq \mathbf{b}_1,$$

where 1_{ij}^c is 1 at the index that corresponds to c_{ij}, 1_{ij}^s is 1 at the index corresponding to s_{ij}, and A_1 and $\mathbf{b}_1$ stack the constraints given in (5) for all i, j.

The decision variables s_{ij} and c_{ij} from (5) show when a bus must start and finish charging, but do not indicate on which charger. The variable $\boldsymbol{\sigma}$ from (2) is a vector of binary variables. Each element of $\boldsymbol{\sigma}$ is denoted σ_{ijk} and is 1 when bus i charges during the jth stop at charger k. Because a bus can only charge at one charger at a time, the values in $\boldsymbol{\sigma}$ must be constrained such that

$$\sum_k \sigma_{ijk} \leq 1 \ \forall i, j \qquad (7)$$

or in standard form as

$$\begin{bmatrix} 1_{ij1} & 1_{ij2} & \dots & 1_{ijk} & 0 & \dots \end{bmatrix} \mathbf{y} \leq \mathbf{1} \ \forall i, j \qquad (8)$$
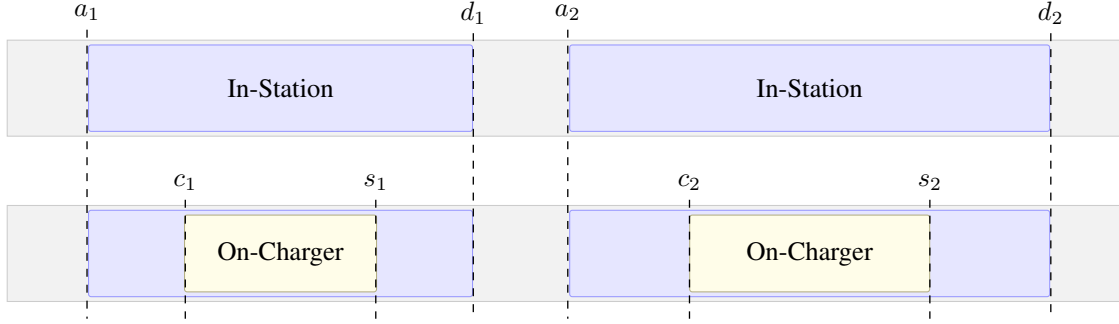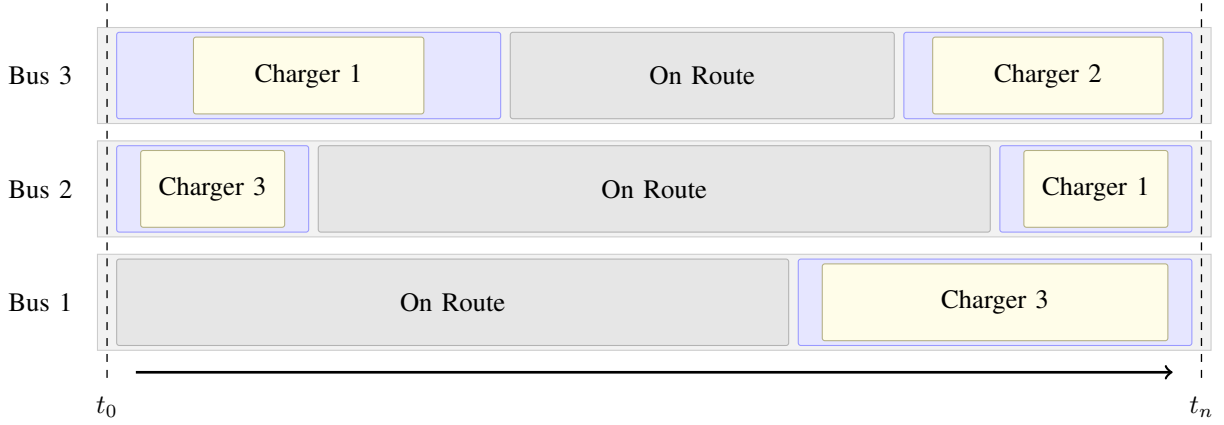$$A_2 \mathbf{y} \leq \mathbf{b}_2,$$

Fig. 1: Bus Charging

Fig. 2: Reserving time slots on chargers

where 1_{ijk} represents a 1 at the location corresponding to σ_{ijk}. The variable σ_{ijk} is used in several scenarios. The first is to ensure that buses without charge assignments have a charge time of zero by constraining s_{ij} and c_{ij} to be the same value. This is done by letting

$$s_{ij} - c_{ij} \leq M \sum_k \sigma_{ijk}$$

$$\begin{bmatrix} 1_s & -1_c & -M_{\sigma_1} & \dots & -M_{\sigma_k} \end{bmatrix} \begin{bmatrix} s_{ij} \\ c_{ij} \\ \sigma_{ij1} \\ \vdots \\ \sigma_{ijk} \end{bmatrix} \leq 0 \ \forall i, j$$

(9)

where M is the maximum difference between s_{ij} and c_{ij}, or the number of seconds in a day, also referred to as nTime, and M_σ represents multiple values of M at locations corresponding to each σ_{ijk}. The constraints in (9) can be appropriately zero padded and stacked for all i, j to form the linear expression

$$A_3 \mathbf{y} \leq \mathbf{b}_3 \qquad (10)$$

The values in $\boldsymbol{\sigma}$, $\mathbf{c}$, and $\mathbf{s}$ form a complete charge plan representation were c_{ij} and s_{ij} describe time periods when a bus will charge and σ_{ijk} gives which charger to use. (see Fig. 2). The variable σ_{ijk} is also necessary to prevent situations where more than one bus is assigned to the same charger at the same time. Note that two buses, bus i and bus i', can only be
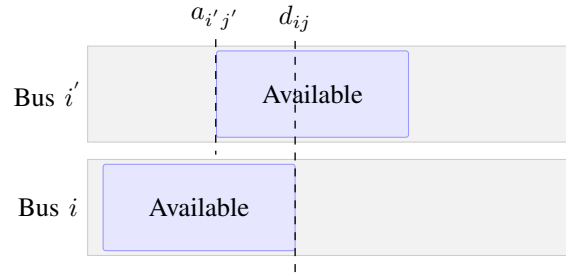

Fig. 3: Potential Overlap

assigned to the same charger at the same time when when a_{ij} for bus i is less than $d_{i'j'}$ for bus i' as shown in Fig. 3. Let $\mathcal{S}$ be the set of all bus-stop pairs such that $\left((i,j), (i',j') \right) \in \mathcal{S}$ if overlap is possible between bus i and bus i' during the j and j' stops respectively. Charging overlap can be avoided by constraining $c_{i'j'} > s_{ij}$ or $c_{ij} > s_{i'j'}$ for all $\left(ij, i'j' \right) \in \mathcal{S}$.

We desire to encode these constraints so that they may be included in our MILP. First, let $l_{(ij, i'j')}$ be a binary decision variable that is 1 when $c_{i'j'} > s_{ij}$, and 0 when $c_{ij} > s_{i'j'}$ so that the overlap constraints can be expressed as

$$c_{i'j'} - s_{ij} > -Ml_{(ij, i'j')}$$
$$c_{ij} - s_{i'j'} > -M(1 - l_{(ij, i'j')})$$

(11)

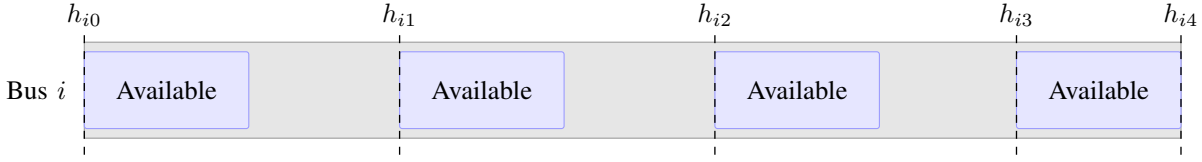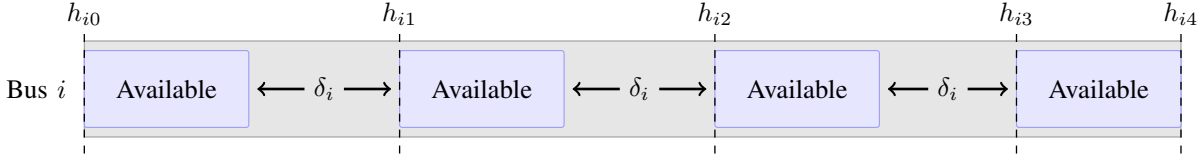Note that this constraint is only necessary when buses i and i'

Fig. 4: State of Charge Variables

Fig. 5: Placement for δ_i

are assigned to the same charger, so that both $\sigma_{i'j'k}$ and σ_{ijk} are equal to 1 which can be done by modifying the switching technique from Eqn. (11) so that the overlap constraints are trivially satisfied when either $\sigma_{i'j'k}$ or σ_{ijk} is equal to zero. The equations in Eqn. (11) can be relaxed by letting

$$c_{i'j'} - s_{ij} > M\left[(\sigma_{i'j'k} + \sigma_{ijk}) - 2\right] - Ml_{(ij,\ i'j')} \ \forall k$$
$$c_{ij} - s_{i'j'} > M\left[(\sigma_{i'j'k} + \sigma_{ijk}) - 2\right] - M(1 - l_{(ij,\ i'j')}) \ \forall k$$
$$(12)$$

so that when $(\sigma_{i'j'k} + \sigma_{ijk}) < 2$, (12) is trivially satisfied for all values of $c_{i'j'}$ and s_{ij} and when $\sigma_{i'j'k} = \sigma_{ijk} = 1$, (12) simplifies to (11). Equation (12) can be expressed in standard form using matrix notation as

$$\begin{bmatrix} -1 & 0 & 0 & 1 & M & M & -M \\ 0 & 1 & -1 & 0 & M & M & M \end{bmatrix} \begin{bmatrix} c_{i'j'} \\ s_{i'j'} \\ c_{ij} \\ s_{ij} \\ \sigma_{i'j'k} \\ \sigma_{ijk} \\ l_{iji'j'} \end{bmatrix} \leq \begin{bmatrix} 2M \\ 3M \end{bmatrix} \forall k$$
$$(13)$$

The constraints in (13) can be repeated for all $\left((i,j), (i',j')\right) \in \mathcal{S}$ and concatenated into a single matrix expression

$$A_4 \mathbf{y} \leq \mathbf{b}_4 \qquad (14)$$

III. BATTERY STATE OF CHARGE

BEBs must also maintain their state of charge above a minimum threshold, denoted $h_{\min}$. Let h_{ij} be the state of charge for bus i at the beginning of stop j as shown in Fig. 4. The initial value for bus i, denoted h_{i0}, is equal to some constant such that

$$h_{i0} = \eta_i \ \forall i$$
$$\begin{bmatrix} 0 & 0 & \dots & 0 & 1_i & 0 \end{bmatrix} \mathbf{y} = \eta_i \ \forall i \qquad (15)$$
$$\tilde{A}_1 \mathbf{y} = \tilde{\mathbf{b}}_1$$

and is otherwise computed as the the sum of incoming and outgoing energy where incoming energy comes from charging, and outgoing energy comes from the battery discharge. The

discharge from operating bus i over route j is denoted δ_{ij} which is assumed to be know ahead of time either from historical data or from modeling such as [29]. The increase in battery state of charge follows a linear charge model such that the increase is equal to the energy rate, denoted p_i, times the time spent charging, denoted Δ_{ij}[30]. The total change from h_{ij} to h_{ij+1} can be expressed as

$$h_{ij+1} = h_{ij} + \Delta_{ij} \cdot p_i - \delta_{ij}. \qquad (16)$$

The value for Δ_{ij} can also be expressed in terms of the difference between a_{ij} and d_{ij} such that

$$h_{ij} + p_i \cdot (s_{ij} - c_{ij}) - \delta_i = h_{ij+1}$$
$$h_{ij+1} - h_{ij} - p_i s_{ij} + p_i c_{ij} = -\delta_i$$
$$\begin{bmatrix} 1 & -1 & -p_i & p_i \end{bmatrix} \begin{bmatrix} h_{ij+1} \\ h_{ij} \\ s_{ij} \\ c_{ij} \end{bmatrix} = -\delta_i \ \forall i,j \qquad (17)$$

The constraints for each i,j outlined in (17) can be vertically concatenated to form

$$A_{ij}\mathbf{y} = \mathbf{b}_{ij} \ \forall i,j$$
$$\tilde{A}_2 \mathbf{y} = \tilde{\mathbf{b}}_2 \qquad (18)$$

Now that the state of charge is defined, the next constraint ensures that the minimum battery state of charge remains both above the minimum threshold, $h_{\min}$, and below the battery capacity, $h_{\max}$. These constraints are given as

$$-h_{ij} \leq -h_{\min}$$
$$h_{ij} \leq h_{\max} \qquad \forall i,j \qquad (19)$$

or

$$\begin{bmatrix} 0 & \dots & 0 & -1_h & 0 & \dots & 0 \\ 0 & \dots & 0 & 1_h & 0 & \dots & 0 \end{bmatrix} \mathbf{y} \leq \begin{bmatrix} h_{\min} \\ h_{\max} \end{bmatrix} \ \forall ij$$
$$A_5 \mathbf{y} \leq \mathbf{b}_5 \qquad (20)$$

The final constraint has to do with the assumption that we desire to use the model for one day to predict the expected cost over a month. To do this, the state of charge at the end of the day must equal the state of charge at the beginning.

Let $h_{i,\text{end}}$ be the final daily state of charge for bus i. This is constrained to be the same as the beginning state of charge as

$$h_{i0} = h_{i,\text{end}} \ \forall i$$
$$h_{i0} - h_{i,\text{end}} = 0 \ \forall i. \tag{21}$$

However, because equality for two continuous variables is computationally demanding, the constraint in (21) can also be expressed as

$$h_{i0} - h_{i,\text{end}} \le 0. \tag{22}$$

Because the final state of charge is dependent on the amount of power used to charge, and power/energy use is penalized (see section V), the optimization process will drive the final state of charge low until it approaches the initial value.

IV. INTEGRATING UNCONTROLLED LOADS

A monthly power bill is made up of several costs, two of which depend on the maximum energy consumed over 15 minutes. This 15-minute average power includes energy that is consumed by loads other than bus chargers, or "uncontrolled loads". In practice, data for uncontrolled loads is sampled and therefore discrete. The representations for how buses use power in Section III are continuous, making their effects difficult to integrate with a discrete uncontrolled load. This section integrates these uncontrolled loads into the planning framework by converting the continuous start and end points, c_{ij} and s_{ij} from Section II, to a vector $\mathbf{p}_{ij}$, where the nth element of the $\mathbf{p}_{ij}$ vector represents the average power over the interval t_{i-1} to t_i from bus i during route j. The route power vectors, $\mathbf{p}_{ij}$, can be added together to form a discrete profile for the buses.

Let the day be divided into time segments, each of duration ΔT. The first step is to determine the index of each segment that a bus begins charging, denoted k_{ij}^{start}, and the index of the segment that a bus finishes charging, denoted k_{ij}^{end}. Each index can be computed as an integer multiple of ΔT that satisfies

$$\begin{aligned} \left(k_{ij}^{\text{start}} - 1\right) \cdot \Delta T + r_{ij}^{\text{start}} &= c_{ij} \\ \left(k_{ij}^{\text{end}} - 1\right) \cdot \Delta T + r_{ij}^{\text{end}} &= s_{ij} \\ k_{ij}^{\text{start}}, k_{ij}^{\text{end}} &\in \mathbb{Z} \\ 0 < r_{ij}^{\text{start}}, r_{ij}^{\text{end}} &< \Delta T. \end{aligned} \tag{23}$$

Equation (23) yields the discrete indices k_{ij}^{start} and k_{ij}^{end} along with corresponding remainder values r_{ij}^{start} and r_{ij}^{end}, which will be used later in this section to calculate the average power for time segments in which buses only charge part of the time. Equation (23) can be rewritten in standard form and zero padded such that

$$\begin{bmatrix} \Delta T & 1 & -1 & 0 & 0 & 0 \\ 0 & 0 & 0 & \Delta T & 1 & -1 \end{bmatrix} \begin{bmatrix} k_{ij}^{\text{start}} \\ r_{ij}^{\text{start}} \\ c_{ij} \\ k_{ij}^{\text{end}} \\ r_{ij}^{\text{end}} \\ s_{ij} \end{bmatrix} = \begin{bmatrix} 0 \\ 0 \end{bmatrix} \ \forall i, j \tag{24}$$

$$\tilde{A}_2 \mathbf{y} = \tilde{\mathbf{b}}_2.$$

and

$$\begin{bmatrix} 0 & -1 & 0 & 0 & 0 & 0 \\ 0 & 1 & 0 & 0 & 0 & 0 \\ 0 & 0 & 0 & 0 & -1 & 0 \\ 0 & 0 & 0 & 0 & 1 & 0 \end{bmatrix} \begin{bmatrix} k_{ij}^{\text{start}} \\ r_{ij}^{\text{start}} \\ c_{ij} \\ k_{ij}^{\text{end}} \\ r_{ij}^{\text{end}} \\ s_{ij} \end{bmatrix} \le \begin{bmatrix} 0 \\ \Delta T \\ 0 \\ \Delta T \end{bmatrix} \ \forall i, j \tag{25}$$

$$A_6 \mathbf{y} \le \mathbf{b}_6.$$

The next step is to use k_{ij}^{start} and k_{ij}^{end} to compute three sets of binary vectors, denoted $\mathbf{g}_{ij}^{\text{start}}$, $\mathbf{g}_{ij}^{\text{on}}$, and $\mathbf{g}_{ij}^{\text{end}}$, which act as selectors for indices which correspond to charge times. The values in $\mathbf{g}_{ij}^{\text{start}}$ and $\mathbf{g}_{ij}^{\text{end}}$ are equal to 1 during intervals that contain energy from the remainders r_{ij}^{start} and r_{ij}^{end}. For example, the values for $\mathbf{g}_{ij}^{\text{start}}$ and $\mathbf{g}_{ij}^{\text{end}}$ from the scenario in Fig. 6b would be

$$\mathbf{g}_{ij}^{\text{start}} = \begin{bmatrix} 1 \\ 0 \\ 0 \\ 0 \end{bmatrix} \text{ and } \mathbf{g}_{ij}^{\text{end}} = \begin{bmatrix} 0 \\ 0 \\ 1 \\ 0 \end{bmatrix}. \tag{26}$$

The values in $\mathbf{g}_{ij}^{\text{on}}$ will be equal to 1 for all time indices where buses charges the entire time. For example, the values in g_{ij}^{on} that correspond to Fig. 6b would be

$$\mathbf{g}_{ij}^{\text{on}} = \begin{bmatrix} 0 \\ 1 \\ 0 \\ 0 \end{bmatrix}. \tag{27}$$

Let $\mathbf{f}$ be a vector of one-based integer indices such that $f_w = w \ \forall w \in (1, \text{nPoint})$, where nPoint is the desired number of discrete samples. For example, if the day was discretized into 4 periods, then $\mathbf{f}$ would be

$$\mathbf{f} = \begin{bmatrix} 1 & 2 & 3 & 4 \end{bmatrix}^T. \tag{28}$$

Defining the index as an element of $\mathbf{f}$ allows us to convert from the single indices k_{ij}^{start} and k_{ij}^{end} to the binary vectors $\mathbf{g}_{ij}^{\text{start}}$ and $\mathbf{g}_{ij}^{\text{end}}$ by letting

$$\begin{aligned} k_{ij}^{\text{start}} &= \mathbf{f}^T \mathbf{g}_{ij}^{\text{start}} \\ k_{ij}^{\text{end}} &= \mathbf{f}^T \mathbf{g}_{ij}^{\text{end}} \\ 1 &= \mathbf{1}^T \mathbf{g}_{ij}^{\text{start}} \\ 1 &= \mathbf{1}^T \mathbf{g}_{ij}^{\text{end}} \\ \mathbf{g}_{ij}^{\text{start}} &\in \{0, 1\}^{\text{nPoint}} \\ \mathbf{g}_{ij}^{\text{end}} &\in \{0, 1\}^{\text{nPoint}}, \end{aligned} \tag{29}$$

which can be expressed in standard form and zero padded to form a set of linear constraints.

$$\begin{bmatrix} 0 & \mathbf{0}^T & -1 & \mathbf{f}^T \\ 0 & \mathbf{1}^T & 0 & 0 \\ -1 & \mathbf{f}^T & 0 & \mathbf{0}^T \\ 0 & 0 & 0 & \mathbf{1}^T \end{bmatrix} \begin{bmatrix} k_{ij}^{\text{start}} \\ \mathbf{g}_{ij}^{\text{start}} \\ k_{ij}^{\text{end}} \\ \mathbf{g}_{ij}^{\text{end}} \end{bmatrix} = \begin{bmatrix} 0 \\ 1 \\ 0 \\ 1 \end{bmatrix} \ \forall i, j \tag{30}$$

$$\tilde{A}_3 \mathbf{y} = \tilde{\mathbf{b}}_3.$$

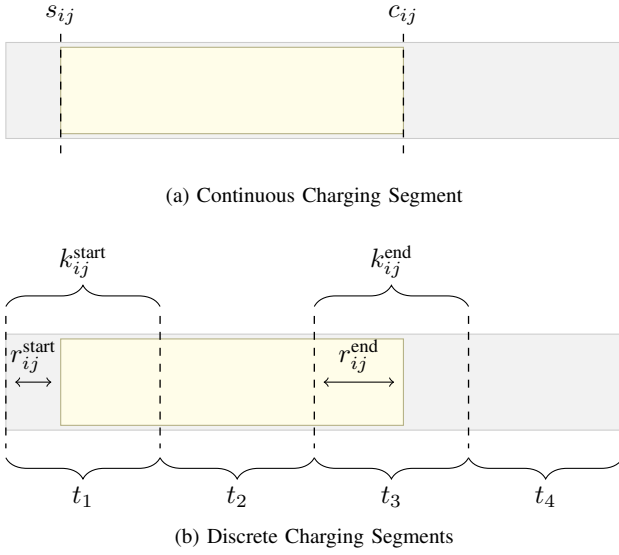The values of $\mathbf{g}_{ij}^{\text{on}}$ can be computed by first noticing that

(a) Continuous Charging Segment

(b) Discrete Charging Segments

Fig. 6: Discretization of continuous charging intervals

indices that correspond to complete charge intervals must remain between k_{ij}^{start} and k_{ij}^{end}, implying that

$$\begin{cases} g_w f_w \leq k^{\text{end}} - 1 \\ g_w f_w \geq k^{\text{start}} + 1 \end{cases} \quad g_w = 1 \,, \tag{31}$$

which can be expressed as a set of linear constraints such that

$$g_w \cdot f_w \leq k_{ij}^{\text{end}} + M(1 - g_w) - 1 \\ g_w \cdot f_w \geq k_{ij}^{\text{start}} - M(1 - g_w) + 1 \tag{32}$$

where M is $2 \cdot \text{nPoint}$. The constraints in (32) do not require that all values between k_{ij}^{start} and k_{ij}^{end} be set to one, rather that them being equal to one implies that they are between k_{ij}^{start} and k_{ij}^{end}. For all values between k_{ij}^{start} and k_{ij}^{end} to be 1, the sum of $\mathbf{g}_{ij}^{\text{on}}$ must be equal to the difference between k_{ij}^{end} and k_{ij}^{start} such that

$$g_w \cdot f_w \leq k_{ij}^{\text{end}} + M(1 - g_w) - 1 \\ g_w \cdot f_w \geq k_{ij}^{\text{start}} - M(1 - g_w) + 1 \\ \mathbf{1}^T \mathbf{g}_{ij}^{\text{on}} = k_{ij}^{\text{end}} - k_{ij}^{\text{start}} - 1. \tag{33}$$

The constraints in (33) work well for a general use case, however when k_{ij}^{end} is equal to k_{ij}^{start}, the last constraint in (33) becomes

$$\mathbf{1}^T \mathbf{g}_{ij}^{\text{on}} = -1. \tag{34}$$

which leads to an empty feasible set because the elements of $\mathbf{g}_{ij}^{\text{on}}$ are all binary. Let k_{ij}^{eq} be a binary variable which is equal to 0 when k_{ij}^{end} is not equal to k_{ij}^{start}. Equation (33) can be modified to incorporate k_{ij}^{eq} to switch between the cases where k_{ij}^{end} is equal, and not equal to k_{ij}^{start} by letting

$$g_w \cdot f_w \leq k_{ij}^{\text{end}} + M(1 - g_w) - 1 \\ g_w \cdot f_w \geq k_{ij}^{\text{start}} - M(1 - g_w) + 1 \\ \mathbf{1}^T \mathbf{g}_{ij}^{\text{on}} = k_{ij}^{\text{end}} - k_{ij}^{\text{start}} - k_{ij}^{\text{eq}}. \tag{35}$$

and constraining k_{ij}^{eq} such that

$$k_{ij}^{\text{end}} - k_{ij}^{\text{start}} - M k_{ij}^{\text{eq}} \leq 0 \\ -k_{ij}^{\text{end}} + k_{ij}^{\text{start}} + M k_{ij}^{\text{eq}} \leq M. \tag{36}$$

The constraints from (35) and (36) can be expressed in standard form as

$$\mathbf{1}^T \mathbf{g}_{ij}^{\text{on}} - k_{ij}^{\text{end}} + k_{ij}^{\text{start}} + k_{ij}^{\text{eq}} = 0 \\ k_{ij}^{\text{end}} - k_{ij}^{\text{start}} - M k_{ij}^{\text{eq}} \leq 0 \\ -k_{ij}^{\text{end}} + k_{ij}^{\text{start}} + M k_{ij}^{\text{eq}} \leq M \tag{37} \\ g_w \left(f_w + M \right) - k_{ij}^{\text{end}} \leq M - 1 \\ g_w \left(M - f_w \right) + k_{ij}^{\text{start}} \leq M - 1.$$

The inequality constraints from equation (37) imply that

$$\begin{bmatrix} f_w + M & -1 & 0 \\ M - f_w & 0 & 1 \end{bmatrix} \begin{bmatrix} g_w \\ k_{ij}^{\text{end}} \\ k_{ij}^{\text{start}} \end{bmatrix} \leq \begin{bmatrix} M - 1 \\ M - 1 \end{bmatrix} \forall g_w \in \mathbf{g}_{ij}^{\text{on}} \tag{38}$$

and that

$$\begin{bmatrix} 1 & -1 & -M \\ -1 & 1 & M \end{bmatrix} \begin{bmatrix} k_{ij}^{\text{end}} \\ k_{ij}^{\text{start}} \\ k_{ij}^{\text{eq}} \end{bmatrix} \leq \begin{bmatrix} 0 \\ M \end{bmatrix} \forall i, j, \tag{39}$$

which can be concatenated for all i, j, and zero padded to form a joint matrix, satisfying

$$A_7 \mathbf{y} \leq \mathbf{b}_7. \tag{40}$$

Similarly, the equality constraint from equation ((37)) can also be concatenated and zero padded such that

$$\mathbf{1}^T \mathbf{g}_{ij}^{\text{on}} - k_{ij}^{\text{end}} + k_{ij}^{\text{start}} + k_{ij}^{\text{eq}} = 0 \ \forall i, j$$

$$\begin{bmatrix} \mathbf{1}^T & -1 & 1 & -1 \end{bmatrix} \begin{bmatrix} \mathbf{g}_{ij}^{\text{on}} \\ k_{ij}^{\text{end}} \\ k_{ij}^{\text{start}} \\ k_{ij}^{\text{eq}} \end{bmatrix} = 0 \tag{41}$$

$$\tilde{A}_4 \mathbf{y} = \tilde{\mathbf{b}}_4.$$

The next step is to define the average power during intervals that only charge for part of the time. These intervals correspond to the remainder values r_{ij}^{start} and r_{ij}^{end} and, as with previous constraints, maintain different behavior when $k_{ij}^{\text{eq}} = 0$ and $k_{ij}^{\text{eq}} = 1$. The average power that corresponds to r_{ij}^{start} and r_{ij}^{end} can be computed as

$$\begin{cases} p_{ij}^{\text{start}} = \dfrac{p \cdot (\Delta T - r_{ij}^{\text{start}})}{\Delta T} & k_{ij}^{\text{eq}} = 1 \\ p_{ij}^{\text{end}} = \dfrac{p \cdot r_{ij}^{\text{end}}}{\Delta T}. & \\ p_{ij}^{\text{start}} = \dfrac{p \cdot \left(r_{ij}^{\text{end}} - r_{ij}^{\text{start}} \right)}{\Delta T} & k_{ij}^{\text{eq}} = 0 \\ p_{ij}^{\text{end}} = 0 & \end{cases} \tag{42}$$

where p is the charge rate. Equation (42) can also be expressed as a set of linear inequality constraints such that

$$
\begin{aligned}
p_{ij}^{\text{start}} &\leq p - \frac{p}{\Delta T} r_{ij}^{\text{start}} + M\left(1 - k_{ij}^{\text{eq}}\right) \\
p_{ij}^{\text{start}} &\geq p - \frac{p}{\Delta T} r_{ij}^{\text{start}} - M\left(1 - k_{ij}^{\text{eq}}\right) \\
p_{ij}^{\text{start}} &\leq \frac{p}{\Delta T} r_{ij}^{\text{end}} - \frac{p}{\Delta T} r_{ij}^{\text{start}} + M k_{ij}^{\text{eq}} \\
p_{ij}^{\text{start}} &\geq \frac{p}{\Delta T} r_{ij}^{\text{end}} - \frac{p}{\Delta T} r_{ij}^{\text{start}} - M k_{ij}^{\text{eq}} \\
p_{ij}^{\text{end}} &\leq \frac{p}{\Delta T} r_{ij}^{\text{end}} + M\left(1 - k_{ij}^{\text{eq}}\right) \\
p_{ij}^{\text{end}} &\geq \frac{p}{\Delta T} r_{ij}^{\text{end}} - M\left(1 - k_{ij}^{\text{eq}}\right) \\
p_{ij}^{\text{end}} &\leq M k_{ij}^{\text{eq}} \\
p_{ij}^{\text{end}} &\geq -M k_{ij}^{\text{eq}},
\end{aligned}
\tag{43}
$$

where M is the battery capacity, and can be expressed in standard form as

$$
\begin{aligned}
p_{ij}^{\text{start}} + \frac{p}{\Delta T} r_{ij}^{\text{start}} + M k_{ij}^{\text{eq}} &\leq M + p \\
-p_{ij}^{\text{start}} - \frac{p}{\Delta T} r_{ij}^{\text{start}} + M k_{ij}^{\text{eq}} &\leq M - p \\
p_{ij}^{\text{start}} - \frac{p}{\Delta T} r_{ij}^{\text{end}} + \frac{p}{\Delta T} r_{ij}^{\text{start}} - M k_{ij}^{\text{eq}} &\leq 0 \\
-p_{ij}^{\text{start}} + \frac{p}{\Delta T} r_{ij}^{\text{end}} - \frac{p}{\Delta T} r_{ij}^{\text{start}} - M k_{ij}^{\text{eq}} &\leq 0 \\
p_{ij}^{\text{end}} - \frac{p}{\Delta T} r_{ij}^{\text{end}} + M k_{ij}^{\text{eq}} &\leq M \\
-p_{ij}^{\text{end}} + \frac{p}{\Delta T} r_{ij}^{\text{end}} + M k_{ij}^{\text{eq}} &\leq M \\
p_{ij}^{\text{end}} - M k_{ij}^{\text{eq}} &\leq 0 \\
-p_{ij}^{\text{end}} - M k_{ij}^{\text{eq}} &\leq 0
\end{aligned}
\tag{44}
$$

and by using matrix multiplication such that

$$
\begin{bmatrix}
1 & 0 & \frac{p}{\Delta T} & 0 & M \\
-1 & 0 & -\frac{p}{\Delta T} & 0 & M \\
1 & 0 & \frac{p}{\Delta T} & -\frac{p}{\Delta T} & -M \\
-1 & 0 & -\frac{p}{\Delta T} & \frac{p}{\Delta T} & -M \\
0 & 1 & 0 & -\frac{p}{\Delta T} & M \\
0 & -1 & 0 & \frac{p}{\Delta T} & M \\
0 & 1 & 0 & 0 & -M \\
0 & -1 & 0 & 0 & -M
\end{bmatrix}
\begin{bmatrix}
p_{ij}^{\text{start}} \\
p_{ij}^{\text{end}} \\
r_{ij}^{\text{start}} \\
r_{ij}^{\text{end}} \\
k_{ij}^{\text{eq}}
\end{bmatrix}
\leq
\begin{bmatrix}
M + p \\
M - p \\
0 \\
0 \\
M \\
M \\
0 \\
0
\end{bmatrix}
\quad \forall i, j
$$
$$
A_8 \leq \mathbf{b}_8
\tag{45}
$$

where p_{ij}^{start}, p_{ij}^{end}, and p represent the average power that corresponds to r_{ij}^{start}, r_{ij}^{end}, and full charging intervals respectively. The total average power use is calculated as

$$
\mathbf{P}_{\text{total}} = \bar{\mathbf{P}}_{\text{load}} + \sum_{ij} \mathbf{g}_{ij}^{\text{start}} \cdot p_{ij}^{\text{start}} + \mathbf{g}_{ij}^{\text{on}} \cdot p + \mathbf{g}_{ij}^{\text{end}} \cdot p_{ij}^{\text{end}}
\tag{46}
$$

where $\bar{\mathbf{P}}_{\text{load}}$ is the average power of the uncontrolled loads.

Note, however that (46) contains the bilinear terms $\mathbf{g}_{ij}^{\text{start}} \cdot p_{ij}^{\text{start}}$ and $\mathbf{g}_{ij}^{\text{end}} \cdot p_{ij}^{\text{end}}$. The expression $\mathbf{g}_{ij}^{\text{start}} \cdot p_{ij}^{\text{start}}$ from (46) can be thought of as a vector, $\mathbf{p}_{ij}^{\text{start}}$ which contains values for p_{ij}^{start} whenever g_{ij}^{start} is not equal to 0 such that

$$
\left.\begin{aligned}
p_w &= p^{\text{start}} & g_w &= 1 \\
p_w &= 0 & g_w &= 0
\end{aligned}\right\} \forall p_w \in \mathbf{p}_{ij}^{\text{start}},
\tag{47}
$$

which can be rewritten as a set of linear inequality constraints such that

$$
\begin{aligned}
p_w &\geq p_{ij}^{\text{start}} - M(1 - g_w) \forall p_w \in \mathbf{p}_{ij}^{\text{start}} \\
p_w &\leq p_{ij}^{\text{start}} + M(1 - g_w) \forall p_w \in \mathbf{p}_{ij}^{\text{start}} \\
p_w &\geq -M g_w \forall p_w \in \mathbf{p}_{ij}^{\text{start}} \\
p_w &\leq M g_w \forall p_w \in \mathbf{p}_{ij}^{\text{start}}
\end{aligned}
\tag{48}
$$

The same approach can be taken to replace $\mathbf{g}_{ij}^{\text{end}} \cdot p_{ij}^{\text{end}}$ with the vector $\mathbf{p}_{ij}^{\text{end}}$ by letting

$$
\begin{aligned}
p_w &\geq p_{ij}^{\text{end}} - M(1 - g_w) \ \forall p_w \in \mathbf{p}_{ij}^{\text{end}} \\
p_w &\leq p_{ij}^{\text{end}} + M(1 - g_w) \ \forall p_w \in \mathbf{p}_{ij}^{\text{end}} \\
p_w &\geq -M g_w \ \forall p_w \in \mathbf{p}_{ij}^{\text{end}} \\
p_w &\leq M g_w \ \forall p_w \in \mathbf{p}_{ij}^{\text{end}},
\end{aligned}
\tag{49}
$$

which can be written in standard form, stacked to accommodate the constraints for all i, j, and zero padded in the usual fashion as

$$
\begin{bmatrix}
-1 & 1 & M \\
1 & -1 & M \\
-1 & 0 & -M \\
1 & 0 & -M
\end{bmatrix}
\begin{bmatrix}
p_w \\
p_{ij}^{\text{start}} \\
g_w
\end{bmatrix}
\leq
\begin{bmatrix}
M \\
M \\
0 \\
0
\end{bmatrix}
\forall p_w \in \mathbf{p}_{ij}^{\text{start}}
\tag{50}
$$
$$
A_9 \leq \mathbf{b}_9.
$$

Equation (49) can be expressed in standard form, stacked for all i, j, and zero padded in a similar fashion such that

$$
\begin{bmatrix}
-1 & 1 & M \\
1 & -1 & M \\
-1 & 0 & -M \\
1 & 0 & -M
\end{bmatrix}
\begin{bmatrix}
p_w \\
p_{ij}^{\text{end}} \\
g_w
\end{bmatrix}
\leq
\begin{bmatrix}
M \\
M \\
0 \\
0
\end{bmatrix}
\forall p_w \in \mathbf{p}_{ij}^{\text{end}}
\tag{51}
$$
$$
A_{10} \mathbf{y} \leq \mathbf{b}_{10}.
$$

An expression for the total power used can then be expressed as

$$
\mathbf{p}^{\text{total}} = \mathbf{p}^{\text{load}} + \sum_{ij} \mathbf{p}_{ij}^{\text{start}} + \mathbf{p}_{ij}^{\text{end}} + \mathbf{g}_{ij}^{\text{on}} \cdot p
\tag{52}
$$

and in standard form as

$$
\begin{bmatrix} 1 & -1^{\text{start}} & -1^{\text{end}} & -1^{\text{on}} \cdot p \end{bmatrix}
\begin{bmatrix}
\mathbf{p}_w^{\text{total}} \\
\mathbf{p}_w^{\text{start}} \\
\mathbf{p}_w^{\text{end}} \\
\mathbf{g}_w^{\text{on}}
\end{bmatrix}
= \mathbf{p}_w^{\text{load}}
\tag{53}
$$
$$
\tilde{A}_4 \mathbf{y} = \tilde{\mathbf{b}}_4
$$

V. OBJECTIVE FUNCTION

This work adopts uses an objective function which implements the rate schedule from [28]. The rate schedule in [28] is based on of two primary components: power and energy.

Power is billed per kW for the highest 15 minute average power over a fixed period of time. It is common practice for power providers to use a higher rate during "on-peak" periods when power is in higher demand and use a lower rate during "off-peak" hours, which account for all other time periods.

The rate schedule given in [28] assesses a fee for a user's maximum average power during on-peak hours, called the On-Peak Power charge, and a user's overall maximum average power, called a facilities charge as shown in figure 7.

	On-Peak	Off-Peak	Both
Energy	On-Peak Energy Charge	Off-Peak Energy Charge	None
Energy Rate	$u_{\text{e-on}}$	$u_{\text{e-off}}$	None
Power	Demand Charge	None	Facilities Charge
Power Rate	$u_{\text{p-on}}$	None	$u_{\text{p-all}}$

Fig. 7: Description of the assumed billing structure

Energy fees are also assessed per kWh of energy consumed with a higher rate for energy consumed during on-peak hours and a lower rate for energy consumed during off-peak hours.

A. Power Charges

It is necessary to compute the maximum power both overall and for on-peak periods. Section IV adopted the convention that ΔT denotes the time offset between power samples and that each power reading would reflect the average power used in the previous interval. Now let us set ΔT to 15 minutes, making $\mathbf{p}_{\text{total}}$ an expression of the 15 minute average power. Next, let $\mathcal{S}_{\text{on}}$ be the set of all indices belonging to on-peak time periods such that $j \in \mathcal{S}_{\text{on}}$ implies that the jth element of $\mathbf{p}^{\text{total}}$, p_j^{total}, represents a 15 minute average during an on-peak interval and let q_{on} be the maximum on-peak average power. With these definitions, constraints for determining the maximum on-peak average are defined as

$$p_j^{\text{total}} \leq q_{\text{on}} \ \forall j \in \mathcal{S}_{\text{on}}$$
$$\begin{bmatrix} 1 & -1 \end{bmatrix} \begin{bmatrix} p_j^{\text{total}} \\ q_{\text{on}} \end{bmatrix} \leq 0 \ \forall j \in \mathcal{S}_{\text{on}} \tag{54}$$
$$A_{11}\mathbf{y} \leq \mathbf{0}$$
$$A_{11}\mathbf{y} \leq \mathbf{b}_{11}$$

Because an increased value in q_{on} is directly related to an increase in cost, the optimizer will minimize q_{on} until it is equal to the maximum value in $\{p_j^{\text{total}} \ \forall j \in \mathcal{S}_{\text{on}}\}$. A similar procedure can be used to derive a set of constraints for the overall maximum average power, denoted q_{all}, and is represented as

$$A_{12}\mathbf{y} \leq \mathbf{0}$$
$$A_{12}\mathbf{y} \leq \mathbf{b}_{12}. \tag{55}$$

The charges for power are then expressed as

$$\text{power cost} = q_{\text{on}} \cdot u_{\text{p-on}} + q_{\text{all}} \cdot u_{\text{p-all}}$$
$$= \begin{bmatrix} u_{\text{p-on}} & u_{\text{p-all}} \end{bmatrix} \begin{bmatrix} q_{\text{on}} \\ q_{\text{all}} \end{bmatrix} \tag{56}$$
$$= \mathbf{u}_{\text{p}}^T \mathbf{y}$$

where $u_{\text{p-on}}$ is the rate per kW for on-peak power use, or the demand charge and $u_{\text{p-all}}$ is the rate per kW for the overall maximum 15 minute average.

B. Energy Charges

Energy is defined as the integral of power over a length of time. Because the values for power given in this work reflect an average power, the energy over a given period can be computed

by multiplying the average power by the change in time, or ΔT such that

$$\text{Total Energy} = \mathbf{1}^T \mathbf{p}_{\text{total}} \cdot \Delta T. \tag{57}$$

However, because the energy is billed for on-peak and off-peak time periods, we define two binary vectors $\mathbf{1}_{\text{on}}$ and $\mathbf{1}_{\text{off}}$ such that $1_j^{\text{on}} = 1 \ \forall j \in \mathcal{S}_{\text{on}}$ and zero otherwise. Similarly, $\mathbf{1}_{\text{off}} = \mathbf{1} - \mathbf{1}_{\text{on}}$. The on-peak and off-peak energy can then be computed as

$$\text{On-Peak Energy} = \mathbf{1}_{\text{on}}^T \mathbf{p}_{\text{total}} \cdot \Delta T$$
$$\text{Off-Peak Energy} = \mathbf{1}_{\text{off}}^T \mathbf{p}_{\text{total}} \cdot \Delta T. \tag{58}$$

Let $u_{\text{e-on}}$ and $u_{\text{e-off}}$ represent the on-peak and off-peak energy rates respectively. The total cost for energy is computed as

$$\text{Energy Cost} = (\mathbf{1}_{\text{on}} \cdot u_{\text{e-on}} \cdot \Delta T)^T \mathbf{p}_{\text{total}} + (\mathbf{1}_{\text{off}} \cdot u_{\text{e-off}} \cdot \Delta T)^T \mathbf{p}_{\text{total}}$$
$$= (\mathbf{u}_{\text{e-on}} + \mathbf{u}_{\text{e-off}})^T \mathbf{p}_{\text{total}}$$
$$= \mathbf{u}_{\text{e}}^T \mathbf{y} \tag{59}$$

C. Cost Function and Final Problem

The entire cost function is given as the sum of the energy and power costs such that

$$\text{Cost} = \mathbf{u}_{\text{p}}^T \mathbf{y} + \mathbf{u}_{\text{e}}^T \mathbf{y}$$
$$= (\mathbf{u}_{\text{p}} + \mathbf{u}_{\text{e}})^T \mathbf{y} \tag{60}$$
$$= \mathbf{v}^T \mathbf{y}$$

The complete problem can now be formulated as

$$\min_{\mathbf{y}} \mathbf{y}^T \mathbf{v} \text{ subject to}$$
$$\tilde{A}_{1:3}\mathbf{y} = \tilde{\mathbf{b}}_{1:3} \ A_{1:12}\mathbf{y} \leq \mathbf{b}_{1:12} \tag{61}$$

or

$$\min_{\mathbf{y}} \mathbf{y}^T \mathbf{g} \text{ subject to}$$
$$\tilde{A}\mathbf{y} = \tilde{\mathbf{b}}, \ A\mathbf{y} \leq \mathbf{b}. \tag{62}$$

VI. RESULTS

This section shows performance for the proposed bus charging algorithm and contains three subsections. Section VI-A compares the proposed method with a previously published algorithm [25].

The comparisons in this section consider a 5 bus, 5 charger scenario with a charge rate of 300 kW. Each solution is expressed in terms of a MILP and solved up to a 2% gap using Gurobi [31], unless otherwise specified. The uncontrolled loads from Section IV are represented with a scaled version of historical data from the Trax Power Substation at UTA. The scaling served to increase the difficulty of the charging problem and better illustrates the capabilities of the proposed algorithm.

A. Cost Comparison with Prior Work

This section compares the monthly cost of energy for the proposed method with three other methods in equivalent 5 bus 5 charger scenarios. The first method is a baseline algorithm that simulates how bus drivers at the Utah Transit Authority (UTA) in Salt Lake City (SLC) charge by default. The second method comes from [24], which was selected because it is very similar to the proposed algorithm, and the third compares with [20] because of how [20] focuses on reducing the instantaneous load from charging. The charge plan for each method is computed using mixed integer linear programs as described below.

Conversations with bus drivers at the UTA in SLC have shown that bus drivers generally top off their batteries whenever a charger is available. In essence, the bus drivers are solving a maximization problem by default as they maximize the number of charge sessions in a day. Hence, the baseline algorithm follows the constraints in Eqn. (61) but incentivizes buses to charge as frequently as possible. Let v_σ^{ijk} be the value of the objective function v at the index corresponding to σ_{ijk} from section II-B. By letting $v_\sigma^{ijk} = -1$, $\forall i, j, k$ and zero otherwise, the baseline method effectively maximizes the number of times a bus can charge. All methods are evaluated according to the rate schedule in [28].

A comparison for each method is given in Fig. 8. Note how the cost of energy is generally the same for each algorithm and that the primary differences in cost come from the on-peak and facilities power charges, illustrating the need to minimize peak average power. To understand the difference in power management between the baseline and the proposed method, refer to Fig. 9. Note how the power for the proposed method (blue line) is almost completely flat, indicating a steady power use. In comparison, the baseline algorithm (red line) is less steady and includes periods of high power use, which leads to the increased power charges in Fig. 8.

A similar phenomena is observed when comparing the proposed method to [24]. Fig. 10 compares the average power for the proposed algorithm and [24]. Note how the proposed algorithm shifts the timing of charging events to produce a charge profile (blue line) that is complementary to the uncontrolled load (tan line). When the uncontrolled load increases the bus load decreases, yielding a flat overall load profile (not shown), whereas the load profile from [24] (red line) shifts charging events to minimize charging during on-peak periods only, but ignores uncontrolled loads. The ability of the proposed method to produce a consistent load profile improves upon [24] because it accounts for the effects of uncontrolled loads and the costs of average power.

B. Scalability

In this section we discuss the limitations for scaling the proposed method with respect to the number of buses. Specifically, we desire to show that the proposed method both performs well with large numbers for buses and can be computed in a reasonable period of time. In Fig. 11, we show how the cost increases with additional buses. Note how the monthly cost of power generally increases by approximately
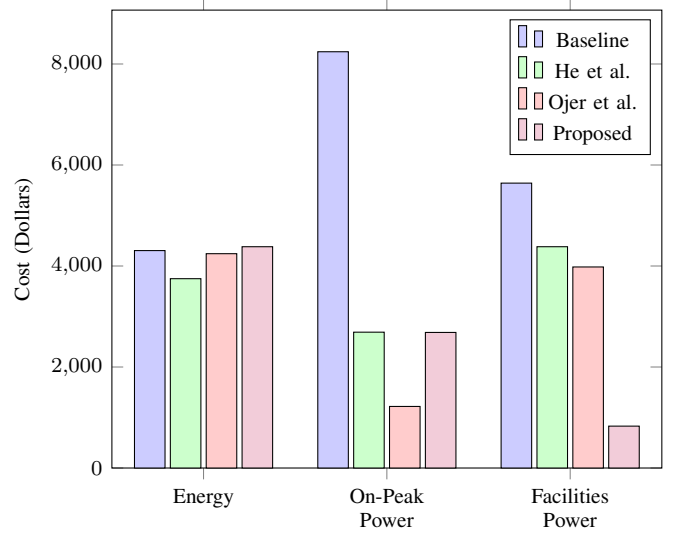

Fig. 8: Cost comparison with prior work

$780 per bus, and that the relationship between cost and bus is linear. This indicates that for each additional bus in the fleet, the added expense comes from energy because the peak loads are intelligently managed. Additionally, the baseline algorithm which refuels buses whenever there is an opportunity reports significant cost increases as the number of buses increase. It is interesting to note how the cost does taper as the bus-to-charger ratio increases, which is not unreasonable as the baseline method does not optimize with respect to cost. The differences between the proposed method and [24] continued to scale as well so the proposed outperformed both the baseline and the method given in [24] in scenarios where there were more buses.

The results for Fig. 12 were obtained by optimizing the monthly cost of 5 to 30 buses up to a 7% gap. Note how the runtime increases significantly as the fleet size increases from 5 to 20 buses and then begins to decrease as the fleet size grows to 30 buses. To understand this behavior, recall that the optimizer is essentially addressing two problems. The first problem is how to schedule charging sessions so that each bus leaves on time and carries sufficient charge. The second problem is to minimize the monthly cost of charging. When the fleet size is small, there are many different charging schedules that meet time and charge constraints and the optimizer has flexibility to select the schedule that minimizes cost. As fleet size increases, the complexity of the scheduling problem increases and this is manifest in increasing runtimes. Past a certain point (above 20 buses in the given scenario) contention for time on the chargers increases and there are fewer charging schedules that meet time and charge constraints. The optimizer has fewer options from which to choose (smaller feasible set) and the optimizer converges more quickly, reducing runtimes.

VII. CONCLUSIONS AND FUTURE WORK

In conclusion, the proposed method yields significant cost savings over the work given in [24], and the default charging behavior at the UTA site. This is accomplished by minimizing
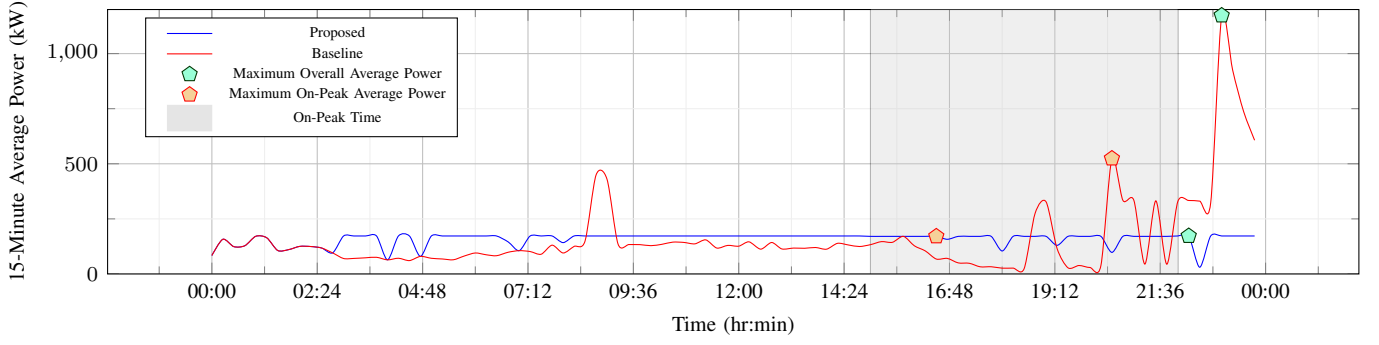
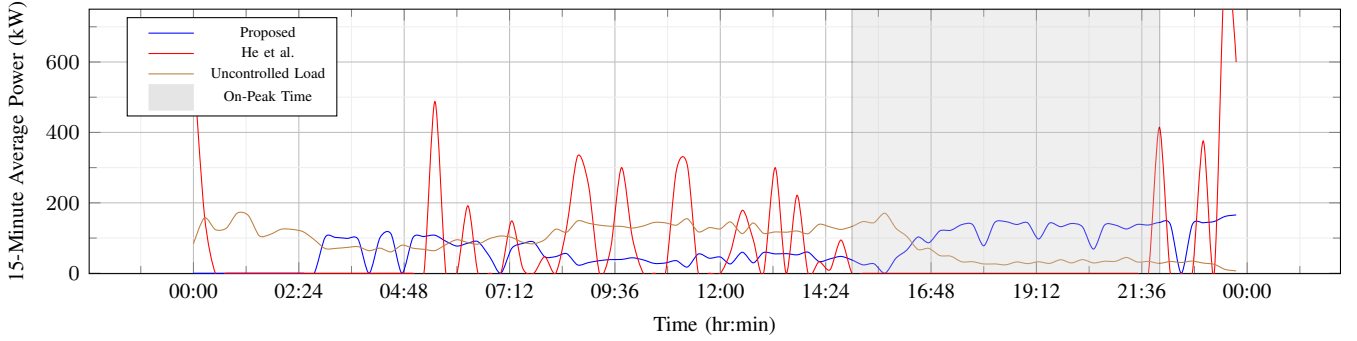Fig. 9: 15-Minute average power for one day

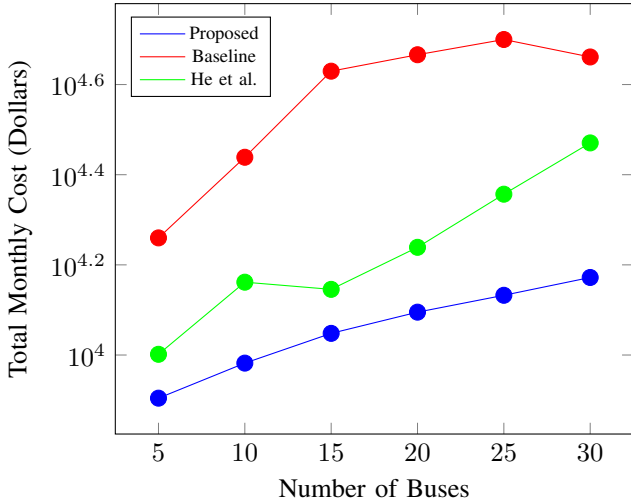Fig. 10: Comparison between uncontrolled and bus loads

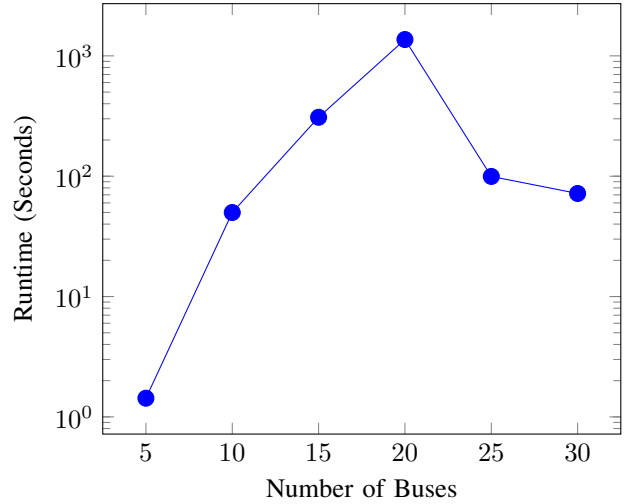Fig. 11: Monthly Cost with 5 Chargers

Fig. 12: Runtime with 5 Chargers at a 7% Gap

on-peak energy, on-peak power, and overall average power in the presence of uncontrolled loads.

Future work might integrate approximate solutions from simpler heuristic approaches to initialize the MILP solver to accelerate convergence. Another known limitation includes how the computational complexity for the current method does not scale with large numbers of buses (more than 30). For larger bus fleets, a decentralized as opposed to a global method might work better.

Finally, this method does not account for uncertainty in the model. Stochastic events such as random arrival times, deviations in actual uncontrolled loads relative to historic values, and uncertainty in battery discharge can significantly affect the usability of the global plan. Accounting for stochastic models of variability can add robustness to the charging solution.

Variable	Description	Range	Variable	Description	Range
Indices					
i	Bus index	$\mathbb{N}$	j	Route index	$\mathbb{N}$
k	Charger index	$\mathbb{N}$			
Route Variables					
a_{ij}	The jth anticipated arrival time of bus i	$\mathbb{R}$	c_{ij}	The start time of the commanded charge window if bus i charges during stop j.	$\mathbb{R}$
s_{ij}	The stop time of the commanded charge window if bus i charges during stop j.	$\mathbb{R}$	d_{ij}	The jth anticipated departure time of bus i.	$\mathbb{R}$
σ_{ijk}	A binary decision variable that is one when bus i charges during stop j at charger k.	$\{0,1\}$	$l_{(ij,i'j')}$	A slack variable that is 1 when bus i uses a charger before bus i' and 0 otherwise.	$\{0,1\}$
$\mathcal{S}$	The set of all pairs $((i,j),(i',j'))$ where bus i and bus j may use the same charger during the j and j' stops respectively.	$(i,j) \times (i',j')$			
State of Charge					
$h_{\min}$	The minimum allowable state of charge	$(0, h_{\max})$	$h_{\max}$	The maximum state of charge	$\mathbb{R}$
η_i	The beginning state of charge for bus i	$(h_{\min}, h_{\max})$	h_{ij}	The state of charge for bus i at the beginning of the jth stop.	$(h_{\min}, h_{\max})$
Δ_{ij}	The time bus i spent charging during the jth stop.	$(h_{\min}, h_{\max})$	p_i	The power at which bus i is charged.	$\mathbb{R}_+$
δ_{ij}	The battery discharge for bus i over route j.	$\mathbb{R}_+$	$h_{i,\text{end}}$	Bus i's final state of charge.	$(h_{\min}, h_{\max})$

Uncontrolled Loads

k_{ij}^{start}	The time index for the start of bus i's j^{th} stop	$\mathbb{Z}$	k_{ij}^{end}	The time index for when bus i disconnects from a charger during it's j^{th} stop.	$\mathbb{Z}$
ΔT	The time difference between each time index.	$\mathbb{R}$	r_{ij}^{start}	The remaining time after c_{ij} has been descritized.	$[0, \Delta T)$
r_{ij}^{end}	The remaining time after s_{ij} has been descritized.	$[0, \Delta T)$	nPoint	the number of desired discrete indices	$\mathbb{Z}$
$\mathbf{g}_{ij}^{\text{start}}$	A binary indicator variable which is one at the k_{ij}^{start} index.	$\{0,1\}^{\text{nPoint}}$	$\mathbf{g}_{ij}^{\text{end}}$	A binary indicator variable which is one at the k_{ij}^{end} index.	$\{0,1\}^{\text{nPoint}}$
$\mathbf{g}_{ij}^{\text{on}}$	A binary indicator variable which is one at each index between k_{ij}^{start} and k_{ij}^{end}.	$\{0,1\}^{\text{nPoint}}$	$\mathbf{f}$	A index vector so that $\mathbf{f}_i = i$ for all integer i between 1 and nPoint.	$\mathbb{Z}^{\text{nPoint}}$
k_{eq}	a binary indicator variable which is one when $k_{ij}^{\text{start}} = k_{ij}^{\text{end}}$.	$\{0,1\}$	p_{ij}^{start}	The average power corresponding to the k_{ij}^{start} time index for bus i's j^{th} stop.	$\mathbb{R}_+$
p_{ij}^{end}	The average power corresponding to the k_{ij}^{end} time index for bus i's j^{th} stop.	$\mathbb{R}_+$	$\mathbf{p}_{ij}^{\text{start}}$	$\mathbf{g}_{ij}^{\text{start}} \cdot p_{ij}^{\text{start}}$	$\mathbb{R}_+^{\text{nPoint}}$
$\mathbf{p}_{ij}^{\text{end}}$	$\mathbf{g}_{ij}^{\text{end}} \cdot p_{ij}^{\text{end}}$	$\mathbb{R}_+^{\text{nPoint}}$	$\mathbf{p}^{\text{load}}$	A vector containing the 15-minute averages for the uncontrolled loads	$\mathbb{R}^{\text{nPoint}}$
$\mathbf{p}^{\text{total}}$	The total 15-minute average power for both the uncontrolled loads and bus chargers.	$\mathbb{R}^{\text{nPoint}}$			

Objective Function

$\mu_{\text{e-on}}$	On-Peak Energy Rate	$\mathbb{R}$	$\mu_{\text{e-off}}$	Off-Peak Energy Rate	$\mathbb{R}$
$\mu_{\text{p-on}}$	On-Peak Demand Power Rate	$\mathbb{R}$	$\mu_{\text{p-all}}$	Facilities Power Rate	$\mathbb{R}$
$\mathcal{S}_{\text{on}}$	The set of on-peak time indices	$\{1, ..., \text{nPoint}\}$	q_{on}	Maximum average power during on-peak periods	$\mathbb{R}$

q_{all}	Maximum average power for all time.	$\mathbb{R}$	$\mathbf{1}_{\text{on}}$	a binary vector which is 1 at the on-peak time indices	$\{0,1\}^{\text{nPoint}}$
$\mathbf{1}_{\text{off}}$	a binary vector which is 1 at the off-peak time indices	$\{0,1\}^{\text{nPoint}}$	$\mathbf{u}_{\text{e-on}}$	a vector of conversion factors from average on-peak power to consumption cost.	$\mathbb{R}^{\text{nPoint}}$
$\mathbf{u}_{\text{e-off}}$	a vector of conversion factors from off-peak average power to consumption cost.	$\mathbb{R}^{\text{nPoint}}$	$\mathbf{u}_e$	a vector of conversion factors from on and off-peak power to consumption cost.	$\mathbb{R}^{\text{nPoint}}$
$\mathbf{u}_p$	A vector of conversion factors from on and off-peak max power to demand cost.	$\mathbb{R}^{\text{nPoint}}$	$\mathbf{v}$	a vector of conversion factors such that $\mathbf{v}^T\mathbf{y}$ yields the total montly cost of power.	$\mathbb{R}^{\text{nPoint}}$

REFERENCES

[1] Moataz Mahmoud et al. "Electric buses: A review of alternative powertrains". In: *Renewable and Sustainable Energy Reviews* 62 (2016), pp. 673–684. DOI: 10.1016/j.rser.2016.05.019.

[2] Kavuri Poornesh, Kuzhivila Pannickottu Nivya, and K. Sireesha. "A Comparative study on Electric Vehicle and Internal Combustion Engine Vehicles". In: *2020 International Conference on Smart Electronics and Communication (ICOSEC)*. 2020, pp. 1179–1183. DOI: 10.1109/ICOSEC49089.2020.9215386.

[3] Hideki Kato et al. "Comparative measurements of the eco-driving effect between electric and internal combustion engine vehicles". In: *2013 World Electric Vehicle Symposium and Exhibition (EVS27)*. 2013, pp. 1–5. DOI: 10.1109/EVS.2013.6914843.

[4] Qifu Cheng et al. "A smart charging algorithm-based fast charging station with energy storage system-free". In: 7.4 (2020), pp. 850–861. DOI: 10.17775/CSEEJPES.2020.00350.

[5] Bálint Csonka. "Optimization of Static and Dynamic Charging Infrastructure for Electric Buses". In: *Energies* 14.12 (2021), p. 3516. DOI: 10.3390/en14123516.

[6] Seog Y. Jeong et al. "Automatic Current Control by Self-Inductance Variation for Dynamic Wireless EV Charging". In: *IEEE Workshop on Emerg. Tech.: Wireless Power Transfer*. June 2018, pp. 1–5. DOI: 10.1109/WoW.2018.8450926.

[7] Bhagyashree J Balde and Arghya Sardar. "Electric Road system With Dynamic Wireless charging of Electric buses". In: *IEEE Trans. Electrification Conf.* 2019, pp. 1–4. DOI: 10.1109/ITEC-India48457.2019.ITECINDIA2019-251.

[8] Yaseen Alwesabi et al. "Robust strategic planning of dynamic wireless charging infrastructure for electric buses". In: *Applied Energy* 230 (2022), p. 120806. DOI: 10.1016/j.energy.2021.120806.

[9] Shubham Jain et al. "Battery Swapping Technology". In: *IEEE Internat. Conf. on Recent Advances and Innovations in Engineering*. 2020, pp. 1–4. DOI: 10.1109/ICRAIE51050.2020.9358366.

[10] Xian Zhang and Guibin Wang. "Optimal dispatch of electric vehicle batteries between battery swapping stations and charging stations". In: *IEEE Power and Energy Society General Meeting*. July 2016, pp. 1–5. DOI: 10.1109/PESGM.2016.7741893.

[11] Nanduni I. Nimalsiri et al. "A Survey of Algorithms for Distributed Charging Control of Electric Vehicles in Smart Grid". In: *IEEE Transactions on Intelligent Transportation Systems* 21.11 (2020), pp. 4497–4515. DOI: 10.1109/TITS.2019.2943620.

[12] Yirong Zhou et al. "Bi-Objective Optimization for Battery Electric Bus Deployment Considering Cost and Environmental Equity". In: *IEEE Trans. on Intel. Transportation Systems* 22.4 (2021), pp. 2487–2497. DOI: 10.1109/TITS.2020.3043687.

[13] Marco Rinalde et al. "Mixed-fleet single-terminal bus scheduling problem: Modeling, solution scheme and potential applications". In: *Omega* 96 (2020), p. 102070. DOI: https://doi.org/10.1016/j.omega.2019.05.006.

[14] Adnane Houbbadi et al. "Optimal Charging Strategy to Minimize Electricity Cost and Prolong Battery Life of Electric Bus Fleet". In: *IEEE Vehicle Power and Propulsion Conf.* 2019, pp. 1–6. DOI: 10.1109/VPPC46532.2019.8952493.

[15] Rong-Ceng Leou and Jeng-Jiun Hung. "Optimal Charging Schedule Planning and Economic Analysis for Electric Bus Charging Stations". In: *Energies* 10.4 (2017). DOI: 10.3390/en10040483.

[16] Ran Wei et al. "Optimizing the spatio-temporal deployment of battery electric bus system". In: *Journal of Transport Geography* 68 (2018), pp. 160,168. DOI: https://doi.org/10.1016/j.jtrangeo.2018.03.013.

[17] Daniel Stahleder et al. "Impact Assessment of High Power Electric Bus Charging on Urban Distribution Grids". In: *IEEE Industrial Electronics Society*. Vol. 1. 2019, pp. 4304–4309. DOI: 10.1109/IECON.2019.8927526.

[18] Sanchari Deb, Karuna Kalita, and Pinakeshwar Mahanta. "Impact of electric vehicle charging stations on reliability of distribution network". In: *IEEE Internat. Conf. on Tech. Adv. in Power and Energy*. 2017, pp. 1–6. DOI: 10.1109/TAPENERGY.2017.8397272.

[19] T. Boonraksa et al. "Impact of Electric Bus Charging on the Power Distribution System a Case Study IEEE 33 Bus Test System". In: *IEEE Grand Internat. Conf. and Exposition Asia*. 2019, pp. 819–823. DOI: 10.1109/GTDAsia.2019.8716023.

[20] Inaki Ojer et al. "Development of energy management strategies for the sizing of a fast charging station for electric buses". In: *IEEE International Conference on Environment and Electrical Engineering*. 2020, pp. 1–6. DOI: 10.1109/EEEIC/ICPSEurope49358.2020.9160716.

[21] Nan Qin et al. "Numerical analysis of electric bus fast charging strategies for demand charge reduction". In: *Trans. Research Part A: Policy and Practice* 94 (2016), pp. 386–396. DOI: 10.17775/CSEEJPES.2020.00350.

[22] Guang Wang et al. "BCharge: Data-Driven Real-Time Charging Scheduling for Large-Scale Electric Bus Fleets". In: *Proceedings - Real-Time Systems Symposium* (2019), pp. 45–55. DOI: 10.1109/RTSS.2018.00015.

[23] Avishan Bagherinezhad et al. "Spatio-Temporal Electric Bus Charging Optimization With Transit Network Constraints". In: *IEEE Transactions on Industry Applications* 56.5 (2020), pp. 5741–5749.

[24] Yi He, Ziqi Song, and Zhaocai Liu. "Fast-charging station deployment for battery electric bus systems considering electricity demand charges". In: *Sustainable Cities and Society* 48 (2019), p. 101530. DOI: https://doi.org/10.1016/j.scs.2019.101530.

[25] Jia He et al. "Battery electric buses charging schedule optimization considering time-of-use electricity price". In: *Journal of Intelligent and Connected Vehicles* 5

(2022), pp. 138–145. DOI: 10.1.108/JICV-03-2022-0006.

[26] Yuhan Liu et al. "Optimal charging plan for electric bus considering time-of-day electricity tariff". In: *Journal of Intelligent and Connected Vehicles* 5 (2022), pp. 123–137. DOI: 10.1108/JICV-03.2022-0008.

[27] Ning Ma and Zhili Zhou. "Mixed-integer Programming Model for Two-dimensional Non-guillotine Bin Packing Problem with Free Rotation". In: *Internat. Conf. for Information Science and Control Engineering*. 2017, pp. 456,460. DOI: 10.1109/ICISCE.2017.102.

[28] Rocky Mountain Power. *Rocky Mountain Power Electric Service Schedule No. 8*. 2021. URL: https://www.rockymountainpower.net/content/dam/pcorp/documents/en/rockymountainpower/rates-regulation/utah/rates/008_Large_General_Service_1_000_kW_and_Over_Distribution_Voltage.pdf.

[29] Jinhua Ji et al. "Trip energy consumption estimation for electric buses". In: *Communications in Transportation Research* 2 (2022), p. 100069. DOI: 10.1016/j.commtr.2022.100069.

[30] Xiaoxue Rong et al. "Coordinated charging strategy of electric vehicle charging station based on combination of linear power flow and genetic algorithm". In: *IEEE Asia-Pacific Power and Energy Engineering Conf.* 2016, pp. 1772–1776. DOI: 10.1109/APPEEC.2016.7779793.

[31] Gurobi Optimization, LLC. *Gurobi Optimizer Reference Manual*. 2022. URL: https://www.gurobi.com.